Proceedings Paper:
Moubark, AM, Harput, S, Cowell, DMJ et al. (2 more authors) (2016) Plane wave imaging challenge. In: IEEE International Ultrasonics Symposium, IUS. 2016 International Ultrasonics Symposium, 18-21 Sep 2016, Tours, France. IEEE . ISBN 9781467398978

https://doi.org/10.1109/ULTSYM.2016.7728893

Plane Wave Imaging Challenge

Asraf Mohamed Moubark, Sevan Harput, David M. J. Cowell, Chris Adams and Steven Freear
Ultrasonics and Instrumentation Group, School of Electronic and Electrical Engineering, University of Leeds, UK.
E-mail: elamm@leeds.ac.uk and S.Freear@leeds.ac.uk

***Abstract*—The plane wave imaging challenge(PICMUS) has been introduced for the first time to IUS in order to encourage participants to compete and share their knowledge in medical ultrasound plane wave imaging. To participate in this challenge, we have chosen the contrast enhanced delay and sum (CEDAS) post signal processing method. This technique have been used to improve B-mode image contrast to noise ratio (CNR) without effecting the image spatial resolution. With CEDAS the energy of every envelope signal is calculated, mapped, and clustered in order to identify the cyst and clutter location. CEDAS significantly reduces the clutter inside the cyst by attenuating it from envelope signals before the new B-Mode image is formed. This paper describes in more details the techniques and parameters we have been using for the challenge. Results obtained for CEDAS shows that it outperforms conventional DAS by 18.33% in experiment and 79.24% in simulation for CNR.**

I. Introduction

Plane wave imaging challenge (PICMUS) is a great opportunity to gain valuable experience by comparing our works with other researchers from all around the world. The same raw simulation and experimental radio frequency (RF) data provided by PICMUS committee must be used by all competitor [1]. Thus performance evaluation measured become standard and can be compared and ranked. At the same time score and ranking from PICMUS also can be used as benchmarking by researchers who participate to evaluate their proposed method. PICMUS provide four different category according to different number of compound plane wave imaging (CPWI), N. Category I is for plane wave imaging (PWI), category II is for CPWI, N=11, category III is for CPWI, N=75 and finally category IV is for arbitrary number of CPWI. Participant can chose one or all four category to participate. We have participated in category three and use our new CEDAS algorithm to process all the data. This has been a good opportunity for us to test the workability of our proposed new method on simulation and experimental data as well. In this paper, we have provided details steps for the method we use to process the raw RF data and present the results in graphical and numerical forms. More details works on CEDAS can be found in [2]

II. Methods

The first step in identifying the location of a cyst and eliminating the clutter inside it starts with calculating the energy of the envelope signal for each of the image lines using the windowing technique [3]. Mapping the envelope signal into energy through the windowing process helps to classify and differentiate from the speckle destructive region and the clutter inside the cyst. Classifying clutter inside the cyst with RF or envelope signals is not feasible. This is because the speckle destructive region produces the same values as the clutter inside cyst.The energy of the envelope signal, G_i calculated from a small segment separately. According to rectangular window size, *N*, G_i is given by following equation:

$$G_i = \sum_{j=0}^{N-1+k} |X_{j+k}|^2 \tag{1}$$

$$i = 1, 2, ..., n; \qquad n = (m - N)/s; \qquad k = 0, s, 2s, ..., ns.$$

Where *X* is number of sample in envelope signal, *i* is number of windowing, *k* is the step increment from one window to another, *s* is an integer even number, *m* is the length of the envelope signal and finally *n* is total number of windowing. All small chunks of energy calculated for each window, G_i are merged so that it becomes one single energy line, E_l as given by

$$E_l = 20\log_{10}\{G_{i=1}(0:s), G_{i=2}(2s:3s), ... \\ ..., G_{i=n}((n-1)s:ns)\} \tag{2}$$

Where l represents the number of imaging lines. Next, before grouping or clustering the energy level into different groups, the transition of the energy level or change in the energy mean are determined. The main objective is to find the most significant changes in the energy level to identify hyperechoic, speckle and hypoechoic region. The highest levels of energy indicate a hyperechoic region. Medium levels of energy indicate speckle region while the lowest energies indicate cyst or hyperechoic regions. Optimal detection of change-points algorithm created by [4] have been used to find the points where the energy signal mean changes most significantly by specifying a minimum residual error improvement in the function. More detailed mathematical works on finding abrupt points can be found in [4] [5]. All changing points, q_{ld} obtained for every energy line, E_l are contained in the following matrix,

$$Q_l = \begin{pmatrix} q_{11} & \cdots & q_{1c} \\ \vdots & \ddots & \vdots \\ q_{x1} & \cdots & q_{xc} \end{pmatrix} \tag{3}$$

$$q_{ld} \in E_l; \qquad d = 1, 2, ..., c.$$

Where the first horizontal direction in the matrix, $Q_{l=1}$ represents all changing points, $(q_{1_1}, q_{1_2}, ..., q_{1_c})$ in the first energy line, $E_{l=1}$ while c represents the total number of changing points.

Once the changing points on the energy signal level are identified for all the lines, they are next grouped or clustered into four different groups by using k-means clustering technique as given by [6]

$$J(a) = \sum_{a=1}^{p} \sum_{l=1}^{x} \parallel Q_l - v_a \parallel^2 \tag{4}$$

$$p < x$$

Where p is the number of clusters and v_a are the centroids for cluster a. The second lowest cluster, $J(a-1)$ was used as a threshold to determine the clutter present. The new envelope signal, $\dot{X}$ was formed for every image line according to the condition stated below

$$\dot{X} = \begin{cases} X, & Q_l \geq J(a-1) \\ \mathrm{X} \times 0.25, & Q_l < J(a-1) \end{cases} \tag{5}$$

New envelope signal formed, $\dot{X}$ is equal to former envelope signal, X if the changing points, Q_l is more than the data inside the second lowest cluster, $J(a-1)$ else X is attenuated by factor of 0.25 if the changing point, Q_l is lower than data inside the second lowest cluster, *J(a-1)*. The new envelope signals are converted into a log scale to form B-Mode image.

III. Simulation and Performance Evaluation

Total set of four different RF data need to be processed with same algorithm in order to obtained the complete results for the image contrast and resolution. Two of the data set obtained from Field II [7] simulation while the other two from CIRS phantom. The simulation and experiments parameters used to obtained the RF data are shown is Table I. A B-mode image was formed with 75 CPWI steered from $-16°$ to $+16°$ with increment of $0.44°$. The window size, N used for the simulation was 4 and the increment size, k is 2. The whole process of calculating the energy from the envelope signal is shown in Fig. 1(a). The variation of speckle formation that is produced from constructive and destructive interference of the scattering signal as can been seen in Fig. 1(b) are now becoming less as in Fig. 1(c).

The energy changing points were sorted from minimum to maximum before they were clustered in order to have better visualisation on the cluster hierarchy. All four clusters are shown in Fig. 2 with their centroids points. Note that the clusters are not in order since k-means assigned centroid points randomly . Thus centroids points are sorted before each one of the cluster identified in order. The lowest clusters are considered as clutter regions and the preceding cluster group is used as the threshold level. In Fig. 2 data in cluster 1 ,red, was used as a threshold. In the case where only two changing points in the energy level are present, the clustering divided whole points into four groups where upper or the top two groups represent the same energy region and the lowest groups represent clutter.

TABLE I
Simulation Parameters

Parameters	Values
Pitch, mm	30
Elements height, mm	5
Sampling Frequencies, MHz	20.832
Centre Frequencies, MHz	5.208
Bandwidth, %	67
No. of Elements	128
Excitation Signal	2.5 cycles

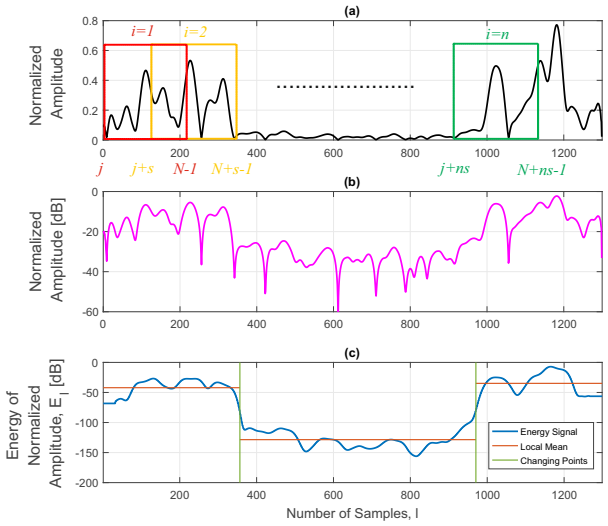

Fig. 1. (a) Energy calculated by applying the windowing technique on the envelope signal. (b) Envelope signal in dB scale. (c) Shows the energy values calculated from (a) mapped into single lines.

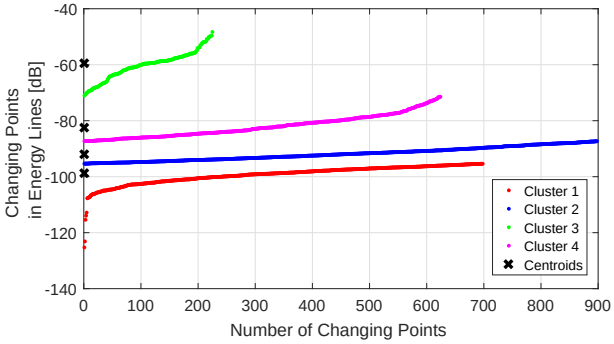

Fig. 2. Cluster assignment for changing points in the energy level.

IV. Performance Evaluation

In order to evaluate the final B-Mode images qualities formed with DAS and CEDAS techniques, CNR is used to measure the cyst contrast with speckle or noise variation inside and outside of the cyst [8]. High CNR value means cyst can be visualize easily and the acoustic noise standard deviation is small or more uniform. CNR equation are given by

$$\text{CNR(dB)} = 20\log_{10}\left(\frac{|\mu_{in} - \mu_{out}|}{\sqrt{({\sigma_{in}}^2 + {\sigma_{out}}^2)/2}}\right) \quad (6)$$

Where μ_{in} and μ_{out} are means of image intensities inside and outside of the cyst respectively while ${\sigma_{in}}^2$ and ${\sigma_{out}}^2$ are their variances. CNR was calculated on the cysts at different depths on the B-Mode images produced by creating two different regions with the same dimensions. The first region is inside the cyst while the other region is located outside the cyst at the same depth. Kolmogoroz-smirnov (KS) test was used to evaluate the speckle quality. The tested region of speckle is considered as positive and no penalty will be applied if α=0.05 or more.

V. Results and Discussions

In this section, performance of both conventional DAS and CEDAS were evaluated qualitatively and quantitatively. Fig. 3, Fig. 4, Fig.5 and Fig. 6 shows qualitative results obtained for DAS and CEDAS with CPWI, N=75 and displayed at 60 dB dynamic range. While Table II gives quantitative results for both technique. The point spread function, PSF obtained from simulation as shown in Fig. 3(a) for DAS and Fig. 3(b) for CEDAS does not show any significant variation between them. This is expected since the proposed technique just focusing in reducing or attenuating clutter noise inside the cyst to increase its contrast.

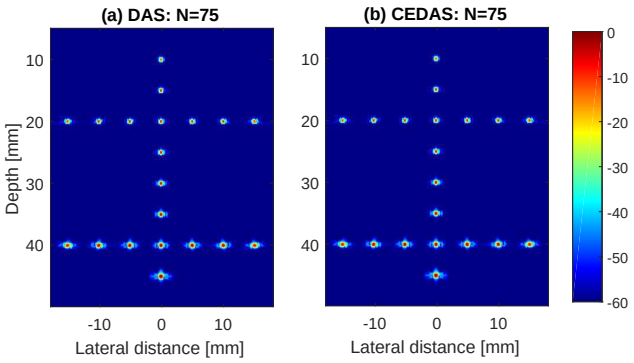

Fig. 3. Field II simulation result for PSF with (a) DAS and (b) CEDAS technique displayed at 60 dB dynamic range and CPWI, N=75.

The B-Mode image obtained from CIRS phantom as shown in Fig. 4 also show that all PSF and lesion information are retain without any changes on them. This is crucial statement in order to prove that the proposed method preserve all the image information without altering them in any forms. However, it can be seen that there is small changes in speckle pattern or variation on both left and right side bottom of the phantom as can be seen in Fig. 4(b). This can be due to area insonified by the L11 probe (Verasonics Inc) not covering equally the scanning region. The variation of speckle formation also can be seen in Fig. 4(a) for DAS as well. The α value obtained through KS test on the speckle variation region gives more than 0.05 value which means the speckle pattern still uniform with less variation.

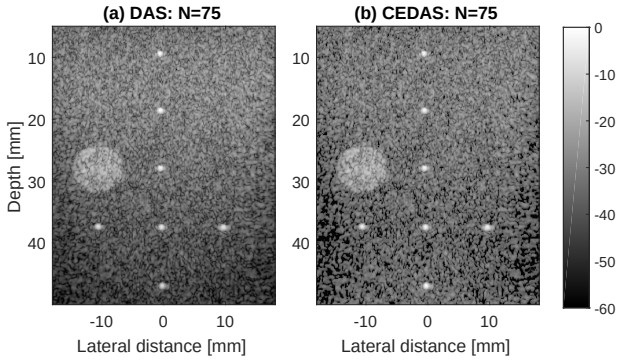

Fig. 4. Experiment result for resolution distortion with (a) DAS and (b) CEDAS technique displayed at 60 dB dynamic range and CPWI, N=75.

B-Mode image of conventional DAS as shown in Fig. 5(a) shows that all nine cysts are effected by clutter noise. On the other hand, the proposed method, CEDAS as shown in Fig. 5(b) successfully detect and attenuated almost all clutter noise that is present inside those cysts. The border also clearly defined. The improvement in Field II simulation also can be seen on B-mode image obtained from CIRS phantom. Fig. 6(b) shows CEDAS outperform DAS by removing all clutter noise inside the cyst leaving the cyst best defined.

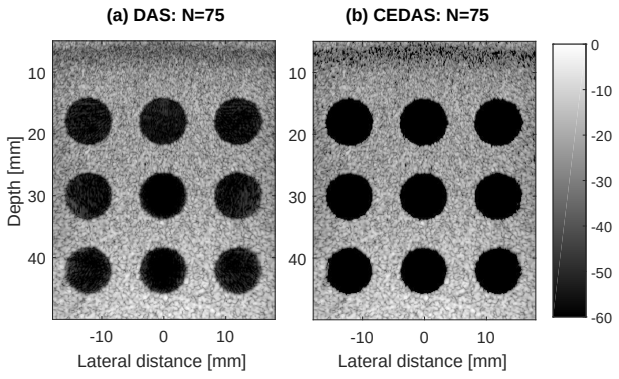

Fig. 5. B-Mode images for (a) DAS, (b) CEDAS displayed at 60 dB dynamic range and CPWI, N=75 for Field II simulation on quantifying the image CNR.

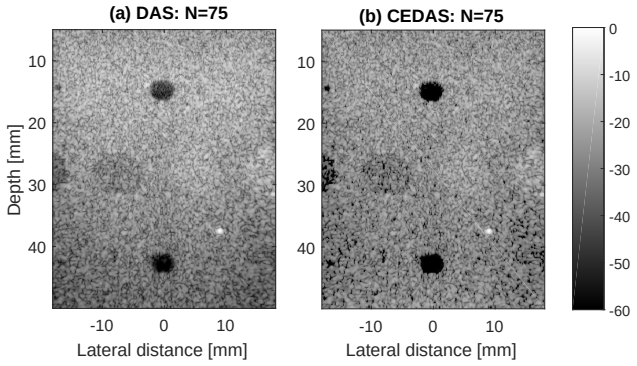

Fig. 6. Experimental result obtained from CIRS for (a) DAS, (b) CEDAS.

The numerical results given in Table II shows that CEDAS outperform DAS in CNR. The average CNR value obtained for CEDAS and DAS through simulation is 27.89 dB and 15.56 dB respectively. The same improvement can be seen on experimental work for CEDAS compared to DAS but with only 2.2 dB gain comparing to 12.33 dB gain in simulation. Since all the speckle formation presertved, no penalty assigned to our result. Average penalty of -40 points will be assigned if there are any reduction in speckle formation or pattern.

TABLE II
RESULTS FOR CONTRAST SPECKLE AND RESOLUTION DISTORTION

Parameters	Experiment		Simulation	
	DAS	CEDAS	DAS	CEDAS
Contrast (dB)	12	14.2	15.56	27.89
Axial Resolution, mm	0.4	0.39	0.56	0.58
Lateral Resolution, mm	0.56	0.34	0.57	0.61
Penalty	0	0	0	0

VI. CONLUSION

The proposed new technique, CEDAS has successfully demonstrated its ability to eliminate clutter inside the cysts phantom for PICMUS challenge. High CNR is achieved by retaining all the B-Mode image properties as in DAS. The CNR for CEDAS improved by 18.33% and 79.24% for experimental and simulation respectively when compared to DAS. A small number of variation, less than 2% was observed on the spatial resolution with CEDAS. Even though this is not expected, further investigation is needed to know the exact reasons. Edge detection on cyst border also has been improved since CEDAS enhanced the contrast level. This can be useful in tracing and marking the edge and border of the cyst. Initial hypothesis was made that the CNR values will be the same for both DAS and CEDAS techniques. However due to less noise variance inside the cyst with CEDAS technique, the CNR value also increase.

REFERENCES

[1] H.Leibgott, A.Rodriguez-Molares, F.Cervenansky, J.A.Jensen, and O.Bernard, "Plane-wave imaging challenge in medical ultrasound," in *Ultrasonics Symposium (IUS), 2016 IEEE International*. IEEE, 2016.

[2] A. M. Moubark, S. Harput, D. MJ, and S. Freear, "Clutter noise reduction in b-mode image through mapping and clustering signal energy for better cyst classification," in *Ultrasonics Symposium (IUS), 2016 IEEE International*. IEEE, 2016.

[3] S. Nisar, O. U. Khan, and M. Tariq, "An efficient adaptive window size selection method for improving spectrogram visualization," *Computational Intelligence and Neuroscience*, vol. 2016, 2016.

[4] R. Killick, P. Fearnhead, and I. Eckley, "Optimal detection of changepoints with a linear computational cost," *Journal of the American Statistical Association*, vol. 107, no. 500, pp. 1590–1598, 2012.

[5] M. Lavielle, "Using penalized contrasts for the change-point problem," *Signal processing*, vol. 85, no. 8, pp. 1501–1510, 2005.

[6] A. Likas, N. Vlassis, and J. J. Verbeek, "The global k-means clustering algorithm," *Pattern recognition*, vol. 36, no. 2, pp. 451–461, 2003.

[7] J. A. Jensen, "Users guide for the field ii program," *Technical University of Denmark*, vol. 2800, 2001.

[8] J. S. Ullom, M. Oelze, and J. R. Sanchez, "Ultrasound speckle reduction using coded excitation, frequency compounding, and postprocessing despeckling filters," in *2010 IEEE International Ultrasonics Symposium*. IEEE, 2010, pp. 2291–2294.